

ALMA Memo 404

Atmospheric Dispersion and Fast Switching Phase Calibration

M.A. Holdaway
National Radio Astronomy Observatory
949 N. Cherry Ave.
Tucson, AZ 85721-0655
email: mholdawa@nrao.edu

J.R. Pardo
Inst. Estructura de la Materia
Dpto. Física Molecular Serrano,
121 Madrid, E-28006 Spain
email: pardo@isis.iem.csic.es

December 19, 2001

Abstract

The differential atmospheric phase of an interferometer has an approximate linear variation with frequency up to about 300 GHz. However, near absorption lines, and especially in the sub-millimeter wavelength atmospheric windows where the absorption lines are very strong and always near, the assumption of a non-dispersive atmosphere breaks down markedly.

We present simulations performed with the ATM atmospheric transmission model (Pardo *et. al.*, 2001), tailored to the specific observing conditions at the Chajnantor site and we propose specific observing strategies to employ for the ALMA telescope. While the *absolute* wet and dry dispersive phase (ie, the part of the phase which deviates from the phase which is linear with ν) can be very large through the atmosphere, the *differential* dispersive phases (ie, the difference in the dispersive phases above two antennas paired in an interferometer) are much smaller. We find that the differential dry atmospheric dispersion is essentially zero at all frequencies of relevance to the ALMA for the expected pressure fluctuations within the area covered by the interferometer. The differential wet dispersion can be large enough to be of concern in the 350, 400-500, 650, and 850 GHz windows.

In fast switching, we expect to observe a calibrator source at 90 GHz and scale the phase solutions to the target frequency. If time dependent wet and dry phase errors occur, ALMA has a potential problem because the wet and dry phases will scale differently with frequency in the sub-millimeter windows. Separation of the phases into wet and dry components may be possible, but this sounds very messy and uncertain, requiring multi-frequency calibrator observations or associated radiometric measurements and good atmospheric modeling. If dry phase errors are negligible and the phase errors can be split between electronic and atmospheric components, then the frequency-dependent phase scaling factor can be determined by a model such as ATM to accurately account for the dispersion. As we do not

have a good handle on the magnitude of dry phase errors, we cannot estimate the success of such a strategy. A worst case scenario would be to assume that the dry phase errors are larger than the dispersive phase. By using the ratio of the frequencies to scale the phase solutions to the target frequency, we correct for the dry errors, but miss the differential wet dispersive phase. The differential wet dispersive phase will manifest itself as some fraction of the phase errors which are just not calibrated. These residual phase errors will be larger during unstable atmospheric conditions, at the edges of the transmission windows, and on longer baselines. During the 10th percentile atmospheric stability conditions, on baselines of 1000 m, the fast switching residual phase will be dominated by the uncompensated dispersive phase at the edges of the sub-millimeter windows (ie, at frequencies where the transmission is less than 50% of the peak transmission for that window). This will markedly affect the ability of fast switching to correct atmospheric phase errors for sub-millimeter observations. Longer baselines could be accommodated by observing during better conditions or by observing near the window center where the dispersive phase is close to zero. If dry phase fluctuations are smaller than the dispersive phase, as will almost certainly occur far from the window centers, the dry phase can be ignored and a correct accounting for the dispersive phase from a transmission model such as ATM can be applied.

If radiometric phase correction were used, a differential dry delay could be quite damaging for sub-millimeter observations. However, if the dry phase were very small, the differential dispersive phase could be calculated from transmission models and applied to correct the phase more perfectly, just as in fast switching with a negligible dry term.

1 Introduction

The current scheme for fast switching phase calibration on the ALMA telescope involves observing a bright calibrator source at 90 GHz with enough sensitivity to scale the phase solution to the target frequency, then quickly slewing to the target source and observing until the phase solution begins to get stale, and then returning to the calibrator source for another phase solution (Holdaway, 2001; Carilli and Holdaway, 1999). There are enough appropriate 90 GHz calibrator sources, the antennas slew and change observing frequency quickly enough, and the atmosphere above Chajnantor is phase stable enough to permit fast switching to work. One of the last big questions for fast switching is: how well will the phase solutions scale from 90 GHz up to the target frequency? Errors in the 90 GHz phase solutions will increase as we scale the phase solutions to the higher frequencies, but the errors due to thermal noise have been included in the fast switching analysis, pushing us toward brighter calibrators, longer calibrator integration times, and more accurate 90 GHz phase solutions when we need to scale the solutions up to higher frequencies. However, we have not yet addressed how the atmospheric phase depends upon frequency. We turn to the ATM atmospheric transmission code to do this.

2 ATM Transmission Code

The ATM (Atmospheric Transmission at Microwaves) package (Pardo, Cernicharo, and Serabyn, 2001) has been developed to provide the radioastronomy and aeronomy communities with an updated tool to compute the atmospheric spectrum in clear-sky conditions for various scientific applications. It calculates atmospheric transmission and phase dispersion accurately for frequencies up to 2 THz, considering line-by-line calculations of all relevant atmospheric species plus empirical wet and dry pseudo-continuum terms which are fit to residuals of FTS measurements between 170 and 1100 GHz. All H₂O lines up to 10 THz are included in order

to correctly account for the entire H₂O far-wing opacity below 2 THz. Although water lines up to 10 THz are included, an extra pseudo-continuum term is still required to fit the data. At this time, the ATM model agrees with measured opacity and transmission data to within one or two percent in the whole range of frequencies to be covered by ALMA and beyond.

The frequency-dependent phase delay function (ie, dispersive phase) is formally related to the absorption line shape via the Kramers-Krönig dispersion theory, and this relation has been used for modeling those delays. Since an empirical pseudo-continuum term is required to fit the opacity data, it is implied that the far wings of the theoretical H₂O line shapes do not perfectly match the actual line shapes. The pseudo-continuum makes no contribution to the dispersive phase, while a treatment with the correct line shape would. However, this contribution to the dispersive phase very far from the H₂O line centers should be extremely small, so we have a fairly high degree of confidence in the ATM calculations of the dispersive phase, though the calculated phase dispersion is purely theoretical and has not been verified experimentally. It is planned that the ATM dispersion calculation will be tested with existing CSO-JCMT interferometer observations combined with simultaneous data from two 3-channel 183 GHz radiometers.

3 Dispersive Phase

We neglect the component of the phase which is linear with frequency (ie, the part of the phase we are usually concerned with) and focus only on the wet and dry dispersive terms (ie, the departures from the phase which is linear with frequency). For 0.5 mm of precipitable water vapor (PWV) on the 5 km high Chajnantor site, the wet dispersive phase is plotted on top of the opacity in Figure 1. Dispersive phase occurs near the water lines, and for 0.5 mm of water, can amount to several hundreds of degrees of phase. There is also dispersion near the narrower dry lines, and the dispersion from atmospheric O₂ lines is shown in Figure 2. Of course, these plots show the dispersive phase caused by the full column of atmosphere above the Chajnantor site. However, for interferometric observations, it is the *differential* dispersive phase that we must be looking at. To the extent the two columns above two different antennas are similar, the dispersive phase will be the same and will cancel when the visibility is formed. Hence, it is only the dispersive phase associated with the *difference* in the atmosphere above the two antennas which will affect the visibility.

The absolute dry dispersive phase is pretty small, generally less than 10 deg within the transparent windows. There will be very little difference in the integrated dry columns above two antennas in the interferometric array, so the *differential* dry dispersion will be the absolute dry dispersion multiplied by the fractional difference in the dry air columns, resulting in a dry dispersive phase which is zero for all practical purposes.

3.1 Estimating the Differential Dispersive Wet Phase

The inhomogeneously distributed water vapor which causes wet phase differences above the two antennas is measured indirectly via the site testing interferometer and is expressed in terms of the phase structure function, so we can accurately estimate the differential wet dispersive phase and its statistics from the archival site testing data (Radford, 2001).

scaling the phase shown in Figure 1 to reflect the difference in the water vapor above two antennas at varying distances and for varying phase stability conditions. The root phase

Percentile	Array Usage	a [deg]	α
5	the best	0.69	0.50
10	850 GHz time	0.91	0.54
20	850 & 650 GHz	1.35	0.56
30	650 & 450 GHz	1.86	0.57
40	350 & 450 GHz	2.46	0.57

Table 1: The 5, 10, 20, 30, and 40% values for the a and α parameters of the root phase structure function: $\sigma_\phi = a(\rho/300)^\alpha$

structure function $\sqrt{D_\phi(\rho)}$ gives the RMS phase error on a baseline of length ρ and is derived from site testing interferometer data taken at 11.2 GHz. It is parameterized as a power law:

$$\sigma_\phi = \sqrt{D_\phi(\rho)} = a(\rho/300)^\alpha, \quad (1)$$

where the values of a and α , determined every 10 minutes, reflect the varying atmospheric phase conditions (Holdaway *et. al*, 1995). The value a reflects the RMS phase over 10 minutes on the site testing interferometer’s 300 m baseline. We convert a to a zenith value by scaling by $\sqrt{\sin(el)}$, where the elevation is 36 deg (Holdaway and Ishiguro, 1995). If a is in degrees, we convert the phase at 11.2 GHz to a path length in millimeters by multiplying by the factor $\lambda_{mm}/360 = 26.78/360$. We convert from the path length difference above two antennas separated by ρ to the water vapor difference above them with the factor $p \simeq 6.3$. Hence, the curve for the absolute wet dispersive phase shown in Figure 1, for 0.5 mm pf water vapor, is converted to the differential wet dispersive phase on a baseline ρ , structure function parameters a and α by the factor

$$2p(26.78/360)\sqrt{\sin(el)}a(\rho/300)^\alpha. \quad (2)$$

The factor of 2 is because the curve in Figure 1 is for only 0.5 mm of PWV. It turns out that the resulting differential dispersive phases are negligible for the millimeter windows for atmospheric conditions on Chajnantor, but become large in the sub-millimeter windows even during the most phase stable conditions. In Figure 4, we plot the differential dispersive phases across the main sub-millimeter windows for the best 10, 20, and 40% atmospheric conditions and for 300, 1000, and 3000 m baselines. The baseline dependence assumes that the phase structure function continues rising with the same exponent at baselines longer than 300 m. This assumption is probably reasonable for the 300 and 1000 m baselines, but overestimates the phases on the 3000 m baseline where the phase structure function exponent has flattened substantially. These plots of the differential dispersive phases for various conditions and baselines will be a guide for when there is a problem and how we can correct for it, which will be discussed below.

In calculating the curves for Figure 4, we used the first two years of site testing data on Chajnantor. The root phase structure function parameters a and α for various atmospheric conditions are given in Table 1.

4 Analysis of Residual Phase Errors Under Fast Switching, Including Dispersion and Dry Phase

Consider two antennas in an interferometer observing a target source T and a calibrator C with fast switching. The target source is observed at a frequency ν_T , the calibrator is observed at a frequency ν_C . The atmospheric phase, in degrees, experienced by the interferometer observing the calibrator will be

$$\phi_C = \Delta w_C \left(360p \frac{\nu_C}{300} + \delta(\nu_C) \right) + \Delta d_C \frac{360}{300} \nu_C, \quad (3)$$

and the atmospheric phase experienced by the interferometer when it observes the target source will be

$$\phi_T = \Delta w_T \left(360p \frac{\nu_T}{300} + \delta(\nu_T) \right) + \Delta d_T \frac{360}{300} \nu_T, \quad (4)$$

where Δw_C is the difference in the water vapor (in mm) above the two antennas in the direction of the calibrator, $w_{C1} - w_{C2}$, Δw_T is the difference in the water vapor in the direction of the target source, the frequencies are measured in GHz such that $300/\nu_C$ gives the wavelength in millimeters, p is the conversion factor from mm of water vapor to mm of path length (about 6.3), $\delta(\nu_C)$ is the frequency dependent dispersive term (in degrees of phase), as calculated from the ATM model for 1 mm of water vapor so $\Delta w_C \delta(\nu_C)$ is the dispersive phase, and Δd_C is the differential dry delay, in mm, for the lines of sight from the antennas to the calibrator. There is a bit of asymmetry in our formulation, as d_C is a delay in mm and w_C is millimeters of water (with an implied delay of $w_C p$), and δ is a phase term.

How do we apply (ie, scale) the phase solution obtained from the calibrator to the target source? We consider three cases:

- **The wet phase is non-dispersive.** For this case, which occurs below 300 GHz or near the centers of the atmospheric windows above 300 GHz, it does not matter if there is a significant dry differential delay or not, as the dry delay is non-dispersive to the accuracy we require. In this case, the calibrator phase should be multiplied by ν_T/ν_C before being applied to the target source as both the wet and dry phase will scale as the frequency. This is what has been assumed about fast switching up until now. Working from Equations 3 and 4, we define ϕ'_T as the calibrator phase scaled by the ratio of the target and calibrator observing frequencies:

$$\phi'_T \equiv \phi_C \frac{\nu_T}{\nu_C} = 1.2\nu_T(p\Delta w_C + \Delta d_C). \quad (5)$$

Then the phase error on the target source is given by

$$\phi_T - \phi'_T = 1.2\nu_T (p(\Delta w_T - \Delta w_C) + (\Delta d_T - \Delta d_C)). \quad (6)$$

Forming the RMS of the phase error, and substituting the time RMS for the ensemble average required for the phase structure function, the entire right hand side is converted into the root phase structure function (including contributions from both nondispersive wet and dry delays) at the target frequency evaluated at some effective calibration baseline $vt/2 + d$ where v is the atmospheric velocity, t is the calibration cycle time, and d (sorry

for overloading this variable’s meaning) is the distance between the lines of site in the atmosphere (Holdaway, 1992; Carilli and Holdaway, 1999):

$$\sigma_\phi = \sqrt{D_\phi(vt/2 + d)}. \quad (7)$$

No atmospheric modeling is required to successfully calibrate this case.

- **The wet phase is dispersive, and there are no dry phase errors.** If the differential dry delay is negligible (ie, if the atmospheric phase error is entirely due to wet turbulence and we are able to remove electronic delays through some method such as the laser-generated calibration tone inserted at the subreflector, as is planned in the ALMA Construction Project Book [2001]), the second term in Equations 3 and 4 above drops out, and the correct scaling of the calibrator phase to the target source phase is given by

$$\frac{1.2p\nu_T + \delta(\nu_T)}{1.2p\nu_C + \delta(\nu_C)}. \quad (8)$$

The success of this method depends on the accuracy of the atmospheric transmission model’s dispersive phase. The dispersive phase as calculated by the transmission model will depend upon the temperature and pressure of the atmosphere, so the state of the atmosphere, including the water vapor profiles, will need to be known to some accuracy. Initial fiddling with ATM’s dispersion calculations suggests that the required accuracy should not be difficult to achieve.

- **The wet phase is dispersive and there are also dry phase errors.** If both a dispersive differential wet delay and a non-dispersive differential dry delay were present, the problem would become very demanding. There is no longer a unique scaling factor which can be applied to the calibrator phases for application at the target frequency. Rather, the wet and dry delays must be solved for independently; the dry delay can be scaled by the ratio of the frequencies, as it is non-dispersive, while the wet delay must be scaled by the model-dependent factor presented in Equation 8. Separating the delay into wet and dry terms would require understanding the dispersive characteristics of the wet and dry terms along with multi-frequency calibration measurements, at a frequency which had no dispersion and at another which displayed marked dispersion. However, the multi-frequency calibration observations would be detrimental to fast switching, requiring a significant portion of the cycle time, thereby reducing the efficiency of the observations. Furthermore, it would be difficult to find a calibrator which is sufficiently strong and close to the target source at a sub-millimeter frequency where the dispersion is sufficiently large to permit separation of delays into wet and dry components. Radiometric and interferometric observations combined could separate the dry and wet phases (assuming the electronic and atmospheric phases could also be separated), but given that the interferometric observations might be required to calibrate the radiometric data, this is an uncertain proposition as well.

5 Estimating Residual Phase Errors Due to Wet Dispersion

As stated above, wet dispersion can be handled easily if the dry phase fluctuations are absent. Similarly, the dry phase errors are no problem for fast switching if there is no dispersion. If

both wet and dry fluctuations are present and they cannot be separated, the best thing that can be done is to determine if the dry phase errors or the wet dispersive phase errors dominate and choose the phase scaling method which results in the smallest scaling error (which is over and above the residual phase error made by fast switching without dispersion).

As the existence and nature of dry phase fluctuations is as yet only hypothetical, we cannot say with certainty at what frequencies and under what conditions the wet dispersion terms dominate or where the dry phase fluctuations dominate. However, a good solid starting point is to look at the magnitude of the wet dispersive phase for various baselines, atmospheric conditions, and frequencies. At some frequencies, such as near the centers of the sub-millimeter windows (see Figure 4 around 675 GHz and 830 GHz) the dispersive phases are close to zero and will be smaller than the dry phase fluctuations (if they exist), and it will make more sense to scale by the ratio of the calibration and target frequencies. In this case, the dispersive phase is unaccounted for and will contribute to the residual phase errors. The level of these unaccounted dispersive phase errors is shown in Figure 4. These errors would add quadratically to the generic residual phase errors from fast switching.

At other frequencies, such as at the edges of the sub-millimeter windows (see Figure 4) the dry phase fluctuations will be smaller than the dispersive phase fluctuations, and it makes more sense to scale by the ratio in Equation 8. In this case, the the residual phase errors will be dominated by the dry phase errors (which scale differently than the wet ones) and errors in the transmission model's dispersive phase estimates (perhaps due to an incomplete knowledge of the physical parameters of the atmosphere). We don't know the extent of the dry turbulence, and a study of the dependence of the dispersive phase on the physical parameters of the atmosphere is beyond the scope of this work. It is expected that many ALMA observations will fall into this regime, and that the additional residual phase errors will actually be smaller than those displayed in Figure 4.

6 Future Work

This work places an upper limit on the residual phase errors caused by dispersive water vapor while employing fast switching phase calibration. Much smaller errors could result if dry phase fluctuations were small. It seems plausible that at some frequencies the dry phase fluctuations will be smaller than the differential wet dispersive phases, and vice versa for other frequencies. These two different regimes imply different phase scaling strategies to minimize the residual phase errors on the target source.

It would be very good to have an understanding of the magnitude of the hypothesized dry phase fluctuations. However, it may very well be that a conclusive answer about the dry phase fluctuations does not come until the ALMA telescope is operational.

Also, an experimental verification of the ATM dispersion calculations should be forthcoming.

Acknowledgments

Thanks to Simon Radford and Jeff Mangum for their helpful suggestions and discussions which were important in untangling the logic behind this memo. Thanks to the entire ALMA Imaging and Calibration group for letting me flip flop for a week until I understood what was really going on.

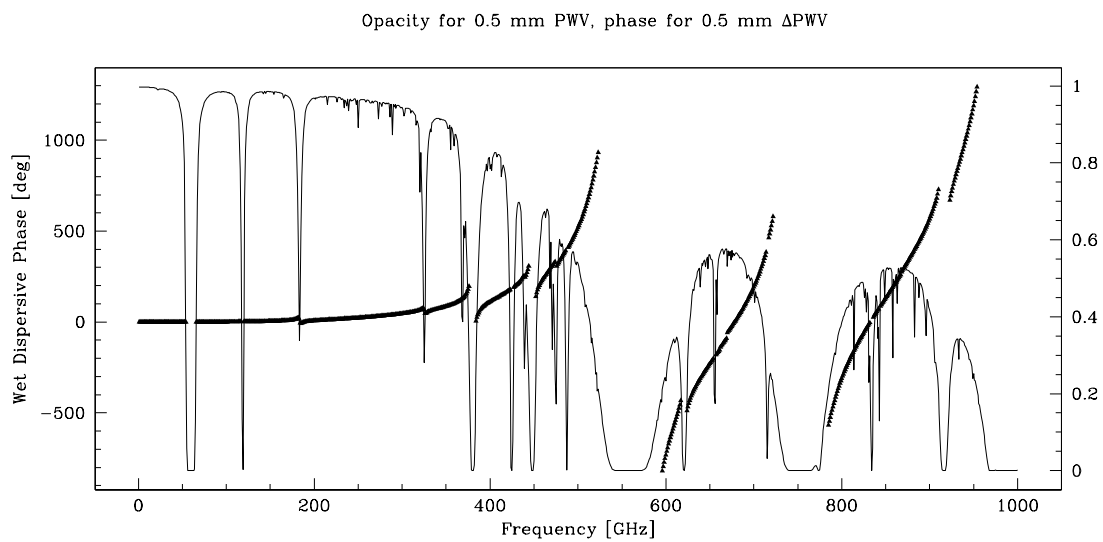


Figure 1: Wet dispersive phase (thick triangles) and opacity for 0.5 mm of PWV above the Chajnantor site.

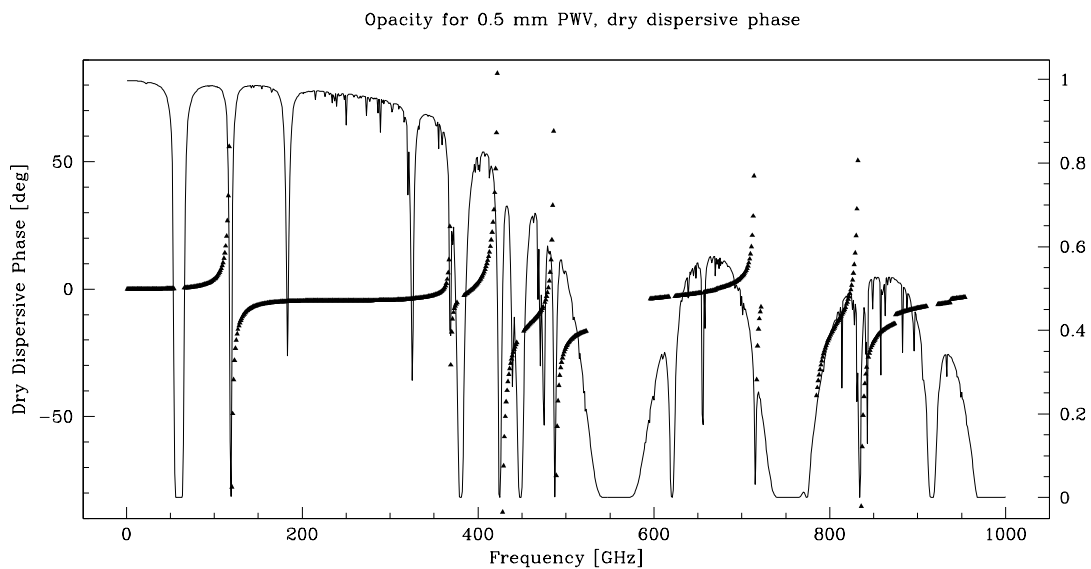


Figure 2: Dry dispersive phase (thick triangles) and opacity for 0.5 mm of PWV above the Chajnantor site.

References

Carilli, C.L., and M.A. Holdaway, “Tropospheric Phase Calibration in Millimeter Interferometry”, ALMA Memo 262, 1999.

“ALMA Construction Project Book”, Chapter 3.2, ed. D. Emerson and J. Baars, 2001.

Holdaway, M.A., “Possible Phase Calibration Schemes for the MMA”, ALMA Memo 84, 1992.

Holdaway, M.A., and Ishiguro, M., “Experimental Determination of the Dependence of Tropospheric Pathlength Variation on Airmass”, ALMA Memo 127, 1995.

Holdaway, M.A., *et. al.*, “Data Processing for Site Test Interferometers”, ALMA Memo 129, 1995.

Holdaway, M.A., “Fast Switching Phase Correction Revisited for 64 12 m Antennas”, ALMA Memo 403, 2001.

Pardo, J.R., J. Cernicharo, and E. Serabyn, “Atmospheric Transmission at Microwaves (ATM): An Improved Model for mm/submm applications” IEEE Trans. on Antennas and Propagation, accepted (Feb. 10, 2001).

Radford, S., “ALMA Site Web Page”, 2001.

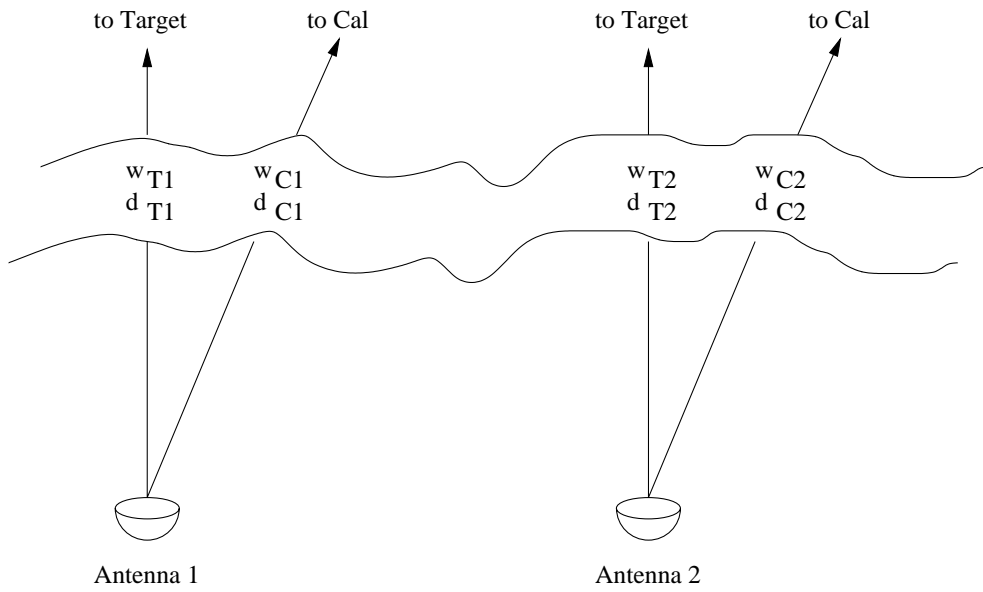


Figure 3: Schematic showing the water vapor columns (*eg*, w_{C1}) and dry delays (*eg*, d_{C1}) toward the calibrator and the target sources above antennas 1 and 2.

Dispersive Phase in Submillimeter Windows: 300 m, 1000 m, 3000 m

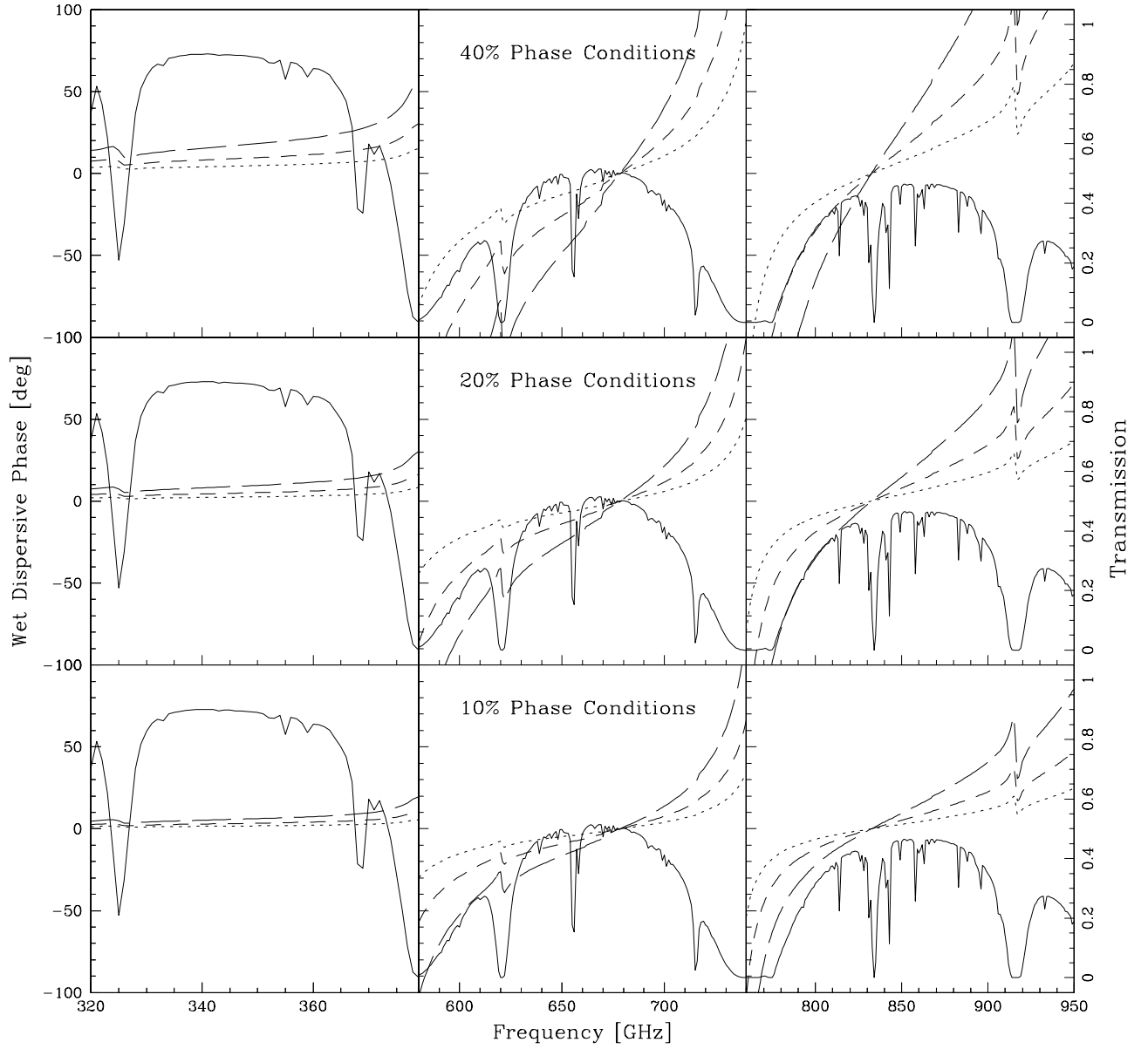


Figure 4: For the 345, 650, and 850 GHz windows, and for the 10% (bottom panels), 20% (middle panels), and 40% (top panels) best phase stability conditions, overlaid on the submillimeter window transparency for 0.62 mm of PWV ($\tau_{225} = 0.035$; solid line), the RMS residual phase due to ignoring the differential wet dispersion on a 300 m (dotted line), a 1000 m (dashed line), and a 3000 m (long dashes) baseline are plotted. The negative phases just reflect the phase dispersion, and the RMS is actually positive.